*J. Nepal Chem. Soc., Vol. 23, 2008/2009*

# The Development of the Intermediate $SnO_2$–$Sb_2O_5$ Layer on Titanium Substrate for Oxygen Evolution Anodes in Seawater Electrolysis

***Jagadeesh Bhattarai****

*Central Department of Chemistry, Tribhuvan Univ., GPO Box 2040, Kathmandu, Nepal*
*e-mail: bhattarai_05@yahoo.com*

## Abstract

*An attempt is made to replace the use of $IrO_2$ by $SnO_2$–$Sb_2O_5$ in the intermediate layer which is necessary to avoid the growth of insulating titanium oxide on the titanium substrate for oxygen evolution γ-$MnO_2$ type $Mn_{1-x-y}Mo_xSn_yO_{2+x}$ anodes in seawater electrolysis. The manganese–molybdenum–tin triple oxides, $Mn_{1-x-y}Mo_xSn_yO_{2+x}$, prepared by anodic deposition on the $SnO_2$–$Sb_2O_5$-coated titanium substrate from $MnSO_4$, $Na_2MoO_4$ and $SnCl_4$ solutions showed around 98.6 % initial oxygen evolution efficiency at a current density of 1000 $Am^{-2}$ in 0.5 M NaCl of pH 1 at room temperature. In order to increase the stability of the anodes, coating at various times to form the intermediate $SnO_2$–$Sb_2O_5$ layer with sufficient thickness on titanium substrate, was performed. The $Mn_{1-x-y}Mo_xSn_yO_{2+x}$ electrodes deposited on the intermediate layer formed from seven times coating showed about 98 % oxygen evolution efficiency after 20 h electrolysis. A small addition of $Sb_2O_5$ to the intermediate layer (that is, $Sb^{5+}/Sn^{4+}$ = 0.124 in the coating solution) seems to be more effective to replace the use of $IrO_2$ for high electronic conductivity and activity of oxygen evolution in seawater electrolysis. The formation of the double oxides of the intermediate $SnO_2$–$Sb_2O_5$ layer after seven times coating seemed responsible for both high conductivity and stability of the $Mn_{1-x-y}Mo_xSn_yO_{2+x}$ anodes.*

***Keywords:*** *$CO_2$ recycling, oxygen evolution electrode, intermediate $SnO_2$-$Sb_2O_5$ layer, seawater electrolysis, titanium substrate.*

## Introduction

The $CO_2$ emissions which induce global warming increase with the growth of the economic activity of the world. Since it is impossible to decrease the

*** Corresponding author***

economic activity, it is also impossible to decrease the $CO_2$ emissions only by efforts for energy saving and by improvements of the energy efficiency. Considering these facts, Hashimoto and his Sendai group of Tohoku University, Japan are proposing effective $CO_2$ recycling to prevent global warming and to supply abundant energy converted from solar energy.[1-8] The most difficult subject in tailoring the key materials necessary for the global $CO_2$ recycling are anode and cathode for seawater electrolysis, and catalyst for $CO_2$ conversion into $CH_4$ from the reaction between $CO_2$ and $H_2$.

For safety production of hydrogen in seawater electrolysis, oxygen production is prerequisite without forming chlorine. In general, seawater electrolysis is practically carried out for chlorine production. Although the equilibrium potential of oxygen evolution is lower than that of chlorine evolution, the chlorine evolution is a simpler reaction than the oxygen evolution, and hence, the formation of chlorine on the anode is generally unavoidable in seawater electrolysis. Nevertheless, for large-scale seawater electrolysis for prevention of global warming, environmentally harmful chlorine release is not allowed. In this context, therefore, one of the most difficult subjects in tailoring key materials for the global $CO_2$ recycling was the anode for seawater electrolysis because, for energy (that is, $CH_4$) production a great quantity of chlorine emissions are not allow, and hence the anode should evolve only oxygen with very high efficiency and durability even in seawater electrolysis at very high current density.

Hashimoto and his co-workers of Sendai group of Japan have tailored many efficient anodes prepared by thermal[9-11] and anodic deposition.[12-16] These anodes were constructed by three layers; the outer layer is the electrocatalyst of γ-$MnO_2$-type double or triple oxides, the intermediate layer is generally 100 % $IrO_2$ and the inner layer is titanium substrate. The $IrO_2$ intermediate layer on titanium substrate was generally formed using the butanolic solution containing 0.52 M $Ir^{4+}$. The $IrO_2$ layer with the same rutile structure as $TiO_2$ was necessary to avoid the formation of insulating titanium oxide on the titanium substrate during anodic polarization at very high current density.

Iridium (IV) oxide is widely used as a dimensionally stable anode (DSA) in various electro-processes because $IrO_2$ acts as the effective anode and has high corrosion resistance among electroanalytically active oxides of platinum group metals. However, in order to supply a future hydrogen demand in the world, the amount of iridium is not sufficient for seawater electrolysis. Therefore, the alternative materials to $IrO_2$ those should have sufficient durability and conductivity at high potentials for anodic polarization, and the same rutile structure as $TiO_2$ are required. Therefore, previous research work of the present author was carried out to decrease in the amount of $IrO_2$ by substitution with $SnO_2$ and increase in the electronic conductivity of the intermediate layer by $Sb_2O_5$ addition to improve the intermediate oxide layer in preventing insulating oxide formation on titanium substrate for oxygen evolution $Mn_{1-x-y}Mo_xSn_yO_{2+x}/IrO_2–SnO_2–Sb_2O_5/Ti$[17-20] and

$Mn_{1-x-y}Mo_xSn_yO_{2+x}/IrO_2–SnO_2/Ti$[19-21] anodes in seawater electrolysis. Because, $SnO_2$ has also the rutile structure as $IrO_2$ and is more stable than $IrO_2$, and hence forms solid solution with $IrO_2$. However, the electronic conductivity of $SnO_2$ is very low as compared to $IrO_2$. Therefore, small amount (about 10%) of $Sb_2O_5$ was added to increase the electronic conductivity of the intermediate layer. Present author has been reported that the anodically deposited γ-$MnO_2$-type $Mn_{1-x-y}Mo_xSn_yO_{2+x}$ anodes on the $IrO_2–SnO_2–Sb_2O_5$–coated titanium substrate containing only about 24 % of the $IrO_2$ showed about 99.7% oxygen evolution efficiency after electrolysis for about 3400 hours in 0.5 M NaCl of pH 1 at 1000 $Am^{-2}$.[18] On the other hand, it has been reported that electrodeposited $Mn_{1-x-y}Mo_xSn_yO_{2+x}$ anodes on the $IrO_2$–coated titanium substrate showed about 100% oxygen evolution efficiency in electrolysis of 0.5 M NaCl of pH 8.4.[16] However, oxygen evolution anodes for seawater electrolysis without $IrO_2$ content in the intermediate oxide layer on the titanium substrate are not reported to the date. In this context, present work is focused to develop the intermediate oxide layer of $SnO_2–Sb_2O_5$ without $IrO_2$.

The present study is aimed to replace completely the amount of $IrO_2$ by tin oxide ($SnO_2$) and antimony oxide ($Sb_2O_5$) addition to increase the electronic conductivity of the intermediate layer in preventing insulating titanium oxide formation on titanium substrate for the oxygen evolution anodes in electrolysis of 0.5 M NaCl of pH 1 at 1000 $Am^{-2}$. The durability of the $Mn_{1-x-y}Mo_xSn_yO_{2+x}/SnO_2$-$Sb_2O_5$/Ti electrodes is also examined.

## Experimental Methods

Punched titanium metal substrate was immersed in a 0.5 M HF solution for 5 min to remove air-formed oxide film, rinsed with de-ionized water and then subjected for surface roughening by etching in 11.5 M $H_2SO_4$ solution at $80^0$C until hydrogen evolution was ceased due to the coverage of the surface by titanium sulfate. Titanium sulfate on the titanium surface was removed by washing under tap water for about 1 hour. Then the etched-titanium sheet was used as substrate for coating of intermediate oxide layer.

Tin (IV) chloride and antimony (V) chloride solutions having the concentration of 0.1 M each were prepared in butanol as stock solutions. The stock solutions of tin (IV) chloride and antimony (V) chloride were mixed to prepare the coating solution for intermediate oxide layer having different amounts of tin and antimony. The ratio of $Sb^{5+}/Sn^{4+}$ in the butanol solution was fixed to 0.124. The coating solution was used for coating on the etched-titanium substrate with a brush, dried at $80^0$C for 10 min, and then baked at $450^0$C for 10 min in air. This coating procedure was repeated for various times so as to form the intermediate oxide layers of $SnO_2–Sb_2O_5$ on titanium substrate. This specimen was finally baked at $450^0$C for 1 h in air. The presence of the $SnO_2–Sb_2O_5$ layer is necessary to prevent the

formation of insulating titanium oxide between electrocatalytically active substances and the titanium substrate during electodeposition and electrolysis of seawater at high current density for a long time. This $SnO_2$–$Sb_2O_5$–coated titanium substrate was cut into 16 x 75 x 1 $mm^3$ as suitable electrode and a titanium wire was spot-welded to its edge. This is called the intermediate oxide layer-coated substrate, that is, $SnO_2$–$Sb_2O_5$/Ti electrode.

The intermediate oxide layer-coated substrate specimen was cleaned by anodic polarization at the current density of 1000 $Am^{-2}$ for 5 min in 10 M NaOH solution and then electroanalytically activated at 1000 $Am^{-2}$ for 5 min in 1 M $H_2SO_4$ solution at room temperature. The $Mn_{1-x-y}Mo_xSn_yO_{2+x}$ anodes were anodically deposited on the clean and activated $SnO_2$–$Sb_2O_5$/Ti substrate at 600 $Am^{-2}$ in the solution containing 0.2 M $MnSO_4.5H_2O$+0.003 M $Na_2MoO_4.2H_2O$+0.006 M $SnCl_4.2H_2O$ at pH -0.1 and $90^0$C for 90 minutes (3 *x* 30 min). The electrodeposition of the $Mn_{1-x-y}Mo_xSn_yO_{2+x}$ anodes was carried out by exchanging fresh electrolyte for every 30 min. The pH of the electrolyte was initially adjusted to -0.1 by adding 18 M $H_2SO_4$. An anode compartment was an alumina cylindrical diaphragm and a cathode was a pair of 316 stainless steel sheets set on the outside of the diaphragm in the cell.

The characterization of the $SnO_2$–$Sb_2O_5$/Ti electrode and the electro-deposited $Mn_{1-x-y}Mo_xSn_yO_{2+x}$/$SnO_2$–$Sb_2O_5$/Ti electrodes were carried out by X-ray diffraction (XRD) with $\alpha$-2$\theta$ mode using $CuK_\alpha$ radiation at a glancing angle $\alpha$ of $5^0$. The changes in the surface morphologies of the $SnO_2$–$Sb_2O_5$/Ti electrode and the electrodeposited $Mn_{1-x-y}Mo_xSn_yO_{2+x}$/$SnO_2$–$Sb_2O_5$/Ti electrodes were observed using confocal scanning laser microscope (CSLM). The laser source used was He-Ne having wavelength of 633 nm.

The oxygen evolution efficiency was measured by electrolysis at constant current density of 1000 $Am^{-2}$ in 0.5 M NaCl solution of pH 1. The amount of oxygen evolved was determined as the difference between the total charge passed and the charge for chlorine formation during electrolysis as described elsewhere.[22] Amount of chlorine formed was analyzed by idiomatic titration of chlorine and hypochlorite.

Galvanostatic polarization curves of the electrodeposited $Mn_{1-x-y}Mo_xSn_yO_{2+x}$ electrodes on the $SnO_2$–$Sb_2O_5$/Ti substrate were measured in 0.5 M NaCl solution of pH 1 at room temperature. The ohmic drop was corrected using a current interruption method. The potential written in this paper hereafter is the overpotential and relative to Ag/AgCl reference electrode with saturated KCl solution.

## Results and Discussion

Figure 1 shows X-ray diffraction patterns of the intermediate oxide layer on the titanium substrate at various coating times using the coating solution containing

the ratio of $Sb^{5+}/Sn^{4+}$ in the intermediate layer is 0.124. The XRD patterns of the intermediate oxide layer on titanium substrate are not same after three and seven times coating. The separate peaks for $SnO_2$, $Sb_2O_5$ with $TiO_2$ are clearly observed at the XRD patterns of the $SnO_2$–$Sb_2O_5$/Ti electrode after three times coating. The sufficient thickness of the intermediate $SnO_2$-$Sb_2O_5$ layer is not gained after three times coating to prevent the formation of insulating titanium oxide on titanium substrate as compared to seven times coating which is clearly observed from the results of the changes in weights of the intermediate layer as a function of coating times (Fig. 2). Consequently, a clear peak for $TiO_2$ observed at the XRD patterns after three times coating. On the other hand, there are no separate peaks for $SnO_2$ and $Sb_2O_5$ in the intermediate oxide layer after seven times coating indicating the formation of single phase of $SnO_2$–$Sb_2O_5$ oxide layer. It is worth mentioning here that tin oxide and antimony oxide were characterized as $SnO_2$ and $Sb_2O_5$, respectively, on the titanium substrate from XPS analysis. The broadening of peaks is clearly observed after seven times coating than that of three times coating. These results revealed that the intermediate $SnO_2$–$Sb_2O_5$ layer on titanium substrate is consisted of a homogeneous double oxide of a single rutile structure with fine grains after seven times coating. By contrast, such double oxide structure of the intermediate $SnO_2$–$Sb_2O_5$ layer is not observed for three times coating one.

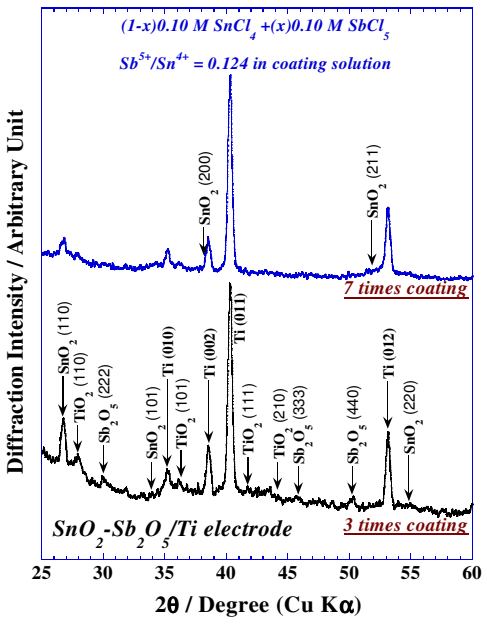


*Figure 1: XRD patterns of the intermediate $SnO_2$-$Sb_2O_5$ layer on the titanium substrate at various coating times.*

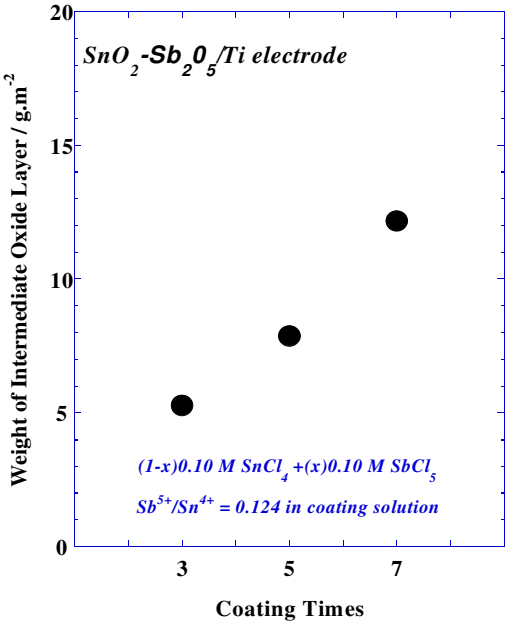


*Figure 2: The change in weight of the intermediate $SnO_2$-$Sb_2O_5$ layer on the titanium substrate as a function of coating time.*

Figure 4 shows the effect of the coating times on the initial oxygen evolution efficiency of the electrodeposited $Mn_{1-x-y}Mo_xSn_yO_{2+x}/SnO_2–Sb_2O_5/Ti$ anodes measured at the current density of 1000 $Am^{-2}$ in 0.5 M NaCl of pH 1 at 25°C. The total concentration of tin and antimony in the coating solution was fixed as 0.1 M and the ratio of $Sb^{5+}/Sn^{4+}$ was 0.124. The initial oxygen evolution efficiency of the $Mn_{1-x-y}Mo_xSn_yO_{2+x}$ anodes deposited on the intermediate oxide layer of $SnO_2–Sb_2O_5$ formed from 3-7 times coating is found in the range of 98.50-99.65%. Furthermore, the durability test on the $Mn_{1-x-y}Mo_xSn_yO_{2+x}/SnO_2–Sb_2O_5/Ti$ anodes after different coating times was carried out with electrolysis times. The increase of coating time of the intermediate $SnO_2–Sb_2O_5$ layer on titanium substrate enhances the durability of the oxygen evolution $Mn_{1-x-y}Mo_xSn_yO_{2+x}/SnO_2–Sb_2O_5/Ti$ anodes as shown in Fig. 4. The anodically deposited $Mn_{1-x-y}Mo_xSn_yO_{2+x}$ electrodes on the $SnO_2–Sb_2O_5/Ti$ layer formed after three and five times coating are stable only for two and 6 h electrolysis, respectively. By contrast, the $Mn_{1-x-y}Mo_xSn_yO_{2+x}$ electrode deposited on the intermediate oxide layer formed after seven times coating is stable for about 20 h electrolysis in 0.5 M NaCl solution and maintains a high oxygen evolution efficiency of about 98.0 % at high the current density. These results revealed that the durability of the $Mn_{1-x-y}Mo_xSn_yO_{2+x}/SnO_2–Sb_2O_5/Ti$ anodes increased with increasing the coating times of the $SnO_2–Sb_2O_5$ layer on titanium substrate and is extend to 20 hours from seven times coating of the $SnO_2–Sb_2O_5/Ti$ layer.

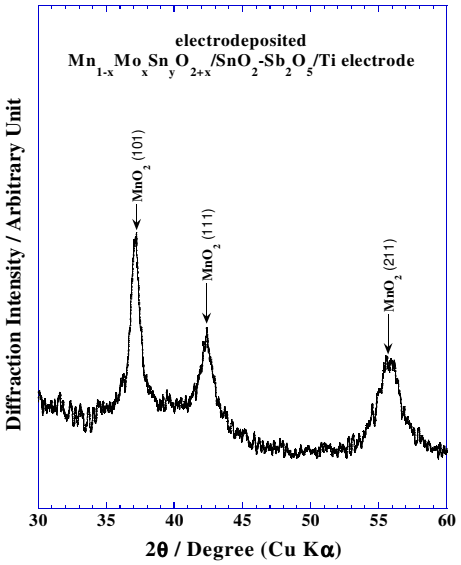


*Figure 3: XRD patterns of the electrodeposited $Mn_{1-x-y}Mo_xSn_yO_{2+x}$ anode on the intermediate $SnO_2–Sb_2O_5$ layer formed after seven times coating on titanium substrate.*

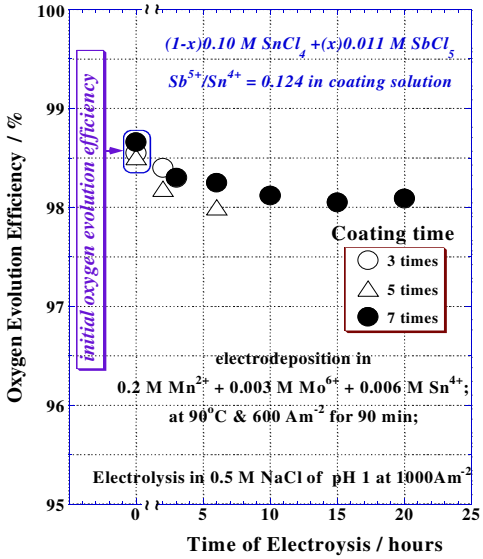


*Figure 4: Changes in the oxygen evolution efficiency of the $Mn_{1-x-y}Mo_xSn_yO_{2+x}/SnO_2–Sb_2O_5/Ti$ electrodes, as a function of electrolysis time.*

Figure 5 shows the changes of the confocal scanning laser microscopic images of the surfaces of $Mn_{1-x-y}Mo_xSn_yO_{2+x}$ oxides on the intermediate layer of $SnO_2$–$Sb_2O_5$ on titanium substrate formed after various coating times. The electrodeposited $Mn_{1-x-y}Mo_xSn_yO_{2+x}$ electrode on three times coated intermediate layer is rather porous and more cracks are observed. With increasing the coating times of the intermediate layer the number of cracks and pores are decreased. In accordance of this change, the durability of the oxygen evolution efficiency of the $Mn_{1-x-y}Mo_xSn_yO_{2+x}$ oxides is increased with coating times of the intermediate $SnO_2$–$Sb_2O_5$ layer on titanium substrate as shown in Fig. 4.

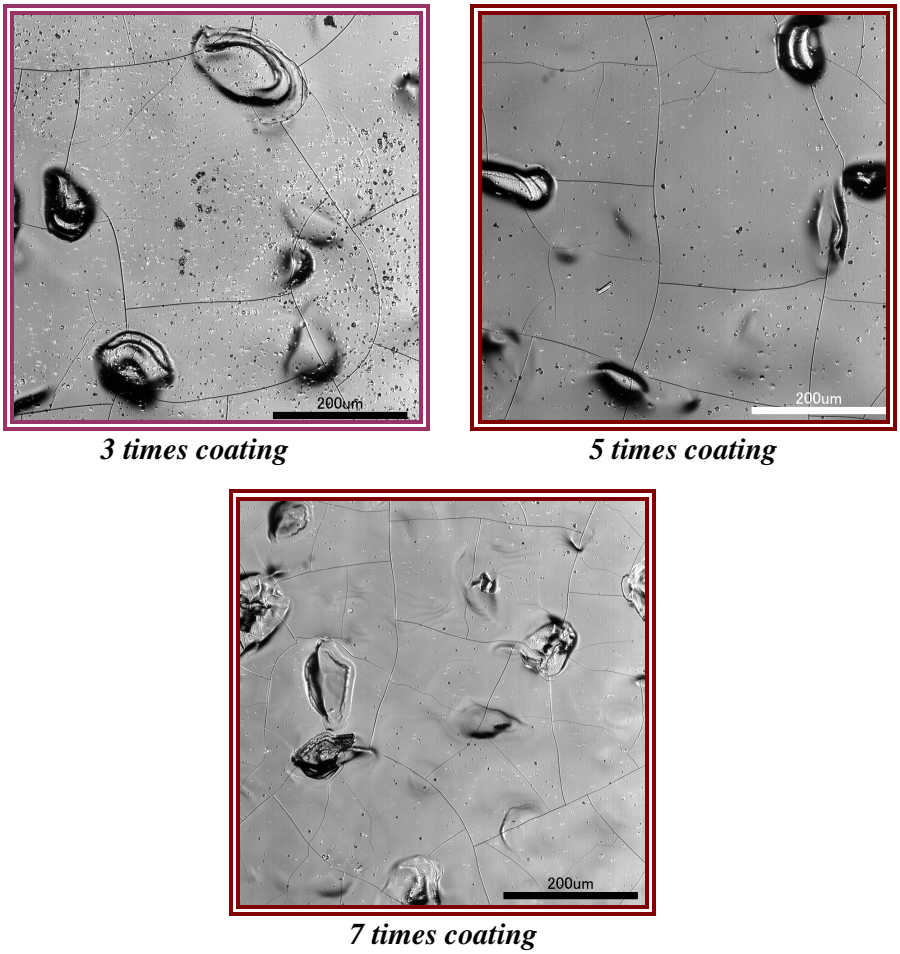


***3 times coating*** ***5 times coating***

***7 times coating***

*Figure 5: Changes in the surface morphology of the electrodeposited* $Mn_{1-x-y}Mo_xSn_yO_{2+x}$*/*$SnO_2$-$Sb_2O_5$*/Ti electrodes, as a function of coating times of the intermediate layer.*

Figure 6 shows IR-corrected galvanostatic polarization curves measured in 0.5 M NaCl solution of pH 1 for the electrodeposited $Mn_{1-x-y}Mo_xSn_yO_{2+x}$ anodes on the $SnO_2$-$Sb_2O_5$ intermediate layer on titanium substrate prepared at various coating times. The polarization curves shift upwards with increasing the coating times. As a result the oxygen overpotentials of the electrodes increase with coating times. In particular, the shifting of polarization curves with coating times is clearly observed at high current density range of 500-1000 $Am^{-2}$. However, the polarization curves at various coating times are almost same at lower current density range of 500 $A.m^{-2}$. The changes in the oxygen overpotentials of the electrodes in 0.5 M NaCl of pH 1 at 1000 $A.m^{-2}$ as a function of coating times is shown in Fig. 7. The oxygen overpotentials of the $Mn_{1-x-y}Mo_xSn_yO_{2+x}/SnO_2–Sb_2O_5/Ti$ anodes deposited on the intermediate oxide layer formed from five and seven times coating are almost the same as that of the 10 % iridium in $IrO_2–SnO_2–Sb_2O_5$ intermediate layer formed from three times coating on titanium substrate as shown in Fig. 7. These results revealed that seven times coating of $SnO_2–Sb_2O_5$ intermediate layer on titanium substrate without $IrO_2$ is necessary to maintain the high electronic conductivity of the intermediate oxide layer of $Mn_{1-x-y}Mo_xSn_yO_{2+x}/SnO_2–Sb_2O_5/Ti$ anodes for seawater electrolysis at high current density.

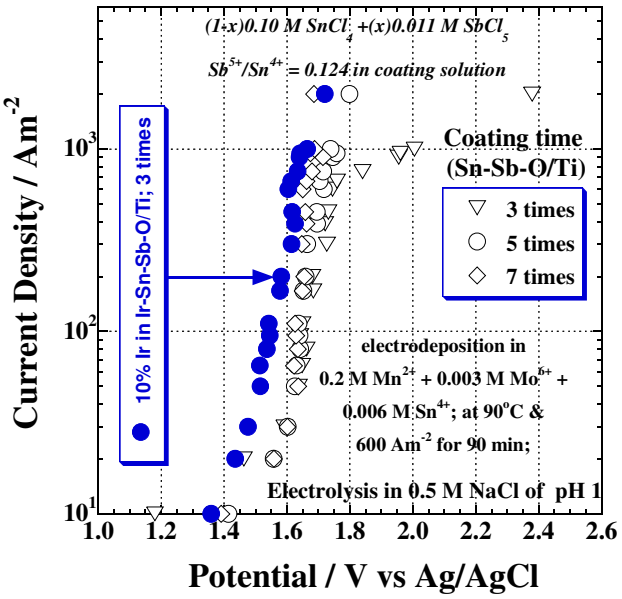


*Figure 6: IR-corrected galvanostatic polarization curves measured in 0.5 M NaCl solution of pH 1 for the electrodeposited $Mn_{1-x-y}Mo_xSn_yO_{2+x}$ anodes on the $SnO_2$-$Sb_2O_5$ intermediate layer on titanium substrate prepared at various coating times. The polarization curve for the anode containing 0.010 M (10%) $Ir^{4+}$ in the Ir-Sn-Sb-O/Ti substrate after 3 times coating is also shown for comparison.*

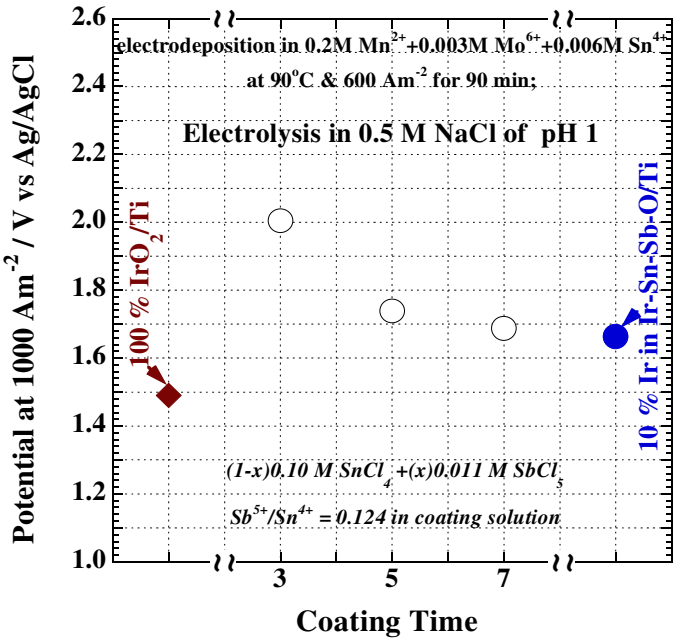


*Figure 7: Change in overpotential at the current density of 1000 A.m$^{-2}$ in 0.5 M NaCl solution of pH 1 for the electrodeposited $Mn_{1-x-y}Mo_xSn_yO_{2+x}$ anodes on the $SnO_2$-$Sb_2O_5$ intermediate layer on titanium substrate prepared at various coating times. The polarization curves for the anodes containing 0.010 M (10%) and 0.100 M (100%) $Ir^{4+}$ in the Ir-Sn-Sb-O/Ti and IrO2/Ti substrates, respectively, after 3 times coating are also shown for comparison.*

## Conclusions

An attempt was made to tailor the intermediate $SnO_2$–$Sb_2O_5$ layer on titanium substrate for oxygen evolution $Mn_{1-x-y}Mo_xSn_yO_{2+x}$ anodes in 0.5 M NaCl of pH 5 at room temperature. Incomplete coverage of the titanium substrate by the intermediate $SnO_2$–$Sb_2O_5$ layer results in short time durability of the anodically deposited $Mn_{1-x-y}Mo_xSn_yO_{2+x}$/$SnO_2$–$Sb_2O_5$/Ti anodes and there has been considerable doubt as to whether the titanium substrate is completely covered by coating only three times because of the XRD reflections of $TiO_2$ is also in the $SnO_2$–$Sb_2O_5$/Ti electrode. The effect of coating repetitions of the intermediate $SnO_2$–$Sb_2O_5$ layer on the oxygen evolution efficiency of the anodes was examined. The durability of the oxygen evolution is increased up to 20 hours when the coating of the intermediate layer was repeated seven times.

## Acknowledgements

The author would like to express his sincere gratitude to Professor Emeritus Dr. Koji Hashimoto and Prof. Dr. Zenta Kato of Tohoku Institute of Technology, Sendai, Japan for providing the research facilities for coatings and XRD. Sincere thanks to Dr. Himendra Jha, Post-doctoral Fellow at the LIMSA, Hokkaido University, Japan for his kind helps for taking the CSLM images.

## References

1. K. Hashimoto, *Mater. Sci. Eng.*, 1994, **A179/A180**, 27-30.
2. K. Hashimoto, *Trans. Mater. Res. Soc. Jpn.*, 1994, **18A**, 35-40.
4. K. Hashimoto, E. Akiyama, H. Habazaki, A. Kawashima, M. Komori, K. Shimamura, N. Kumagai, *Sci. Rep. Res. Inst. Tohoku Univ.*, 1997, **A4**, 153.
5. K. Hashimoto, M. Yamasaki, K. Fujimura, T. Matsui, K. Izumiya, M. Komori, A. A. Al-Moneim, E. Akiyama, H. Habazaki, N. Kumagai, A. Kawashima, K. Asami, *Mater. Sci. Eng.*, 1999, **A267**, 200-206.
6. K. Hashimoto, H. Habazaki, M. Yamasaki, S. Meguro, S. Sasaki, H. Katagiri, T. Matsui, K. Fujimura, K. Izumiya, N. Kumagai and E. Akiyama, *Mater. Sci. Eng.*, 2001, **A304-306**, 88-96.
7. K. Hashimoto, M. Yamasaki, S. Meguro, S. Sasaki, H. Katagiri, K. Izumiya, N. Kumagai, H. Habazaki, E. Akiyama, K. Asami, *Corros. Sci.*, 2002, **44**, 371-386.
8. K. Hashimoto, in *Corrosion and Electrochemistry of Advanced Materials; Electrochemical Soc. Transactions*, 2006, **1(4)**, 533.
9. K. Izumiya, E. Akiyama, H. Habazaki, N. Kumagai, A. Kawashima, K. Asami, K. Hashimoto, *J. Appl. Electrochem.*, 1997, **27**, 1362-1368.
10. K. Izumiya, E. Akiyama, H. Habazaki, N. Kumagai, A. Kawashima, K. Asami, K. Hashimoto, *Mater. Trans. (JIM)*, 1997, **38**, 899-905.
11. K. Izumiya, E. Akiyama, H. Habazaki, N. Kumagai, A. Kawashima, K. Asami, K. Hashimoto, *Mater. Trans. (JIM)*, 1998, **39**, 308.
12. K. Izumiya, E. Akiyama, H. Habazaki, N. Kumagai, A. Kawashima, K. Asami, K. Hashimoto, *Electrochim. Acta*, 1998, **43**, 3303-3312.
13. K. Fujimura, K. Izumiya, A. Kawashima, H. Habazaki, E. Akiyama, N. Kumagai, K. Hashimoto, *J. Appl. Electrochem.*, 1999, **29**, 765-771.
14. K. Fujimura, T. Matsui, K. Izumiya, N. Kumagai, E. Akiyama, H. Habazaki, A. Kawashima, K. Asami, K. Hashimoto, *Mater. Sci. Eng.*, 1999, **A267**, 254-259.
15. H. Habazaki, T. Matsui, A. Kawashima, K. Asami, N. Kumagai, K. Hashimoto, *Script. Mater.*, 2001, **44**, 1659-1662.

16. N. A. Abdel Ghany, N. Kumagai, S. Meguro, K. Asami and K. Hashimoto, *Electrochim. Acta*, 2002, **48**, 21-28.
17. J. Bhattarai, H. Shinomiya, Z. Kato, K. Izumiya, N. Kumagai and K. Hashimoto, *in Proc. 54th Japan Conf. Materials and Environments*, Japan Society of Corrosion Engineers, Hiroshima, Japan. 2007, **C-207**, 345-348.
18. Z. Kato, J. Bhattarai, K. Izumiya, N. Kumagai and K. Hashimoto, in *Abstract volume of 214th the Electrochemical Society Meeting-2008, October*. **Abstract No. 1623** and *Electrochemical Soc. Transactions*, in press (2009).
19. J. Bhattarai, in Abstract; *International Chemical Congree-2008*, Nepal Chemical Society, Kathmandu, Nepal. 2008, **Abstract No. EG-06**, p. 39.
20. J. Bhattarai, *J. Nepal Chem. Soc.*, 2008/2009, **23**, 21.
21. J. Bhattarai, H. Shinomiya, Z. Kato, K. Izumiya, N. Kumagai and K. Hashimoto, *in Extended Abstract, Joint Meeting of the Electrochemical Society of Japan and Japan Society of Corrosion Engineers*, Sapporo, Japan. 2008, **Abstract No. 206**, p. 27.
22. N. Kumagai, Y. Samata, A. Kawashima, K. Asami, K. Hashimoto, *J. Appl. Electrochem.*, 1987, **17**, 347.
23. B. D. Cullity, in *Elements of X-ray Diffraction*, 2nd edition, Addison-Wesley Publ. Co, Inc., 1977, p.101.